Effects of island geometry in postdeposition island growth

Oana Tataru and Fereydoon Family
Department of Physics, Emory University, Atlanta, Georgia 30322

Jacques G. Amar
Department of Physics and Astronomy, University of Toledo, Toledo, Ohio 43606
(Received 4 October 1999; revised manuscript received 2 February 2000)

The results of kinetic Monte Carlo simulations of a realistic model of postdeposition island growth that takes into account the spatial extent of islands are presented. Simulations were carried out on one- and two-dimensional substrates for different values of the critical island size i and were compared with previous results for a point-island model. The use of a realistic island geometry results in enhanced island aggregation and coalescence. This leads to an increase in the average island size S as well as the exponent z describing the dependence of S on coverage. The shape of the island-size distribution for $i=3$ also changes dramatically due to the existence of ''magic'' islands.

I. INTRODUCTION

Numerous recent experimental and theoretical studies have been aimed at a better understanding of the formation and growth of thin films. In the early stages of growth, the main processes that play a role are the deposition and diffusion of adatoms and the formation and growth of islands by nucleation, aggregation, and coalescence. Understanding how the island density n and island-size distribution n_s, where n_s is the density of islands of size s, are influenced by these atomic-scale competing processes is an essential first step in describing thin-film growth.

One of the key parameters in submonolayer growth is the ratio D/F of the adatom hopping rate D to the deposition rate F, which is typically much larger than 1. Accordingly, a great deal of recent experimental[1–11] and theoretical[12–22] work has focused on the dependence of these quantities on the deposition flux as well as on the critical island size i corresponding to one less than the number of atoms in the smallest stable cluster. While in typical conditions of molecular beam epitaxy (MBE) D/F is quite large (i.e., $D/F=10^5-10^{11}$), in some cases (i.e., at relatively low temperatures and large deposition fluxes) this ratio may be quite small (i.e., $D/F \leqslant 1$). In this case, because of the rapid deposition flux compared to the diffusion, island nucleation and growth occur primarily after deposition has occurred rather than during deposition. In this regime, which we refer to as postdeposition nucleation, the primary factors affecting the island density and distribution are the total coverage deposited and the critical island size i.[15] The study of this regime is motivated by several thin-film growth experiments[23–25] in which the flux of adatoms was shut off and the surface either quenched from a high temperature, or allowed to relax before a subsequent layer was deposited.

In this paper we report the results of kinetic Monte Carlo simulations of postdeposition nucleation. We note that, recently, Li, Rojo, and Sander[26] have carried out kinetic Monte Carlo simulations of a point-island model of postdeposition nucleation in order to study the effects of critical island size and substrate dimension on the scaling of the island density and size distribution with coverage. In their model, the islands are assumed to be points, i.e., they occupy only one lattice site, and cannot grow in extent. While such a model is valid in the limit of very low coverage ($\theta \ll 1$) for which the average island size is much less than the typical separation between islands, for larger coverages the finite size of the islands may play a crucial role due to both coalescence and the increased capture number of large islands. Accordingly, we have carried out kinetic Monte Carlo simulations of postdeposition nucleation using a more realistic model corresponding to extended islands. To study the effects of substrate dimension and temperature on the island growth process, simulations were carried out for different values of the critical island size i and on both one- and two-dimensional substrates. In order to study the scaling behavior, the dependence of the average island size on coverage and the scaling of the island-size distribution were investigated and compared with previous results for a point-island model.

The outline of this paper is as follows. In Sec. II we discuss our model and contrast it with the point-island model. In Sec. III we present our results, which show the effects of island geometry in postdeposition nucleation. We discuss our results and present our conclusions in Sec. IV.

II. MODEL AND SIMULATIONS

In our model, adatoms were first deposited randomly onto the substrate with coverage θ. In order to study the surface evolution during postdeposition nucleation, adatoms that were not part of a stable cluster were then allowed to diffuse via nearest-neighbor hops until every atom was part of a stable cluster, as determined by the critical island size i. In particular, for the case $i=1$, corresponding to a stable dimer, an atom with one nearest-neighbor bond was assumed to be immobile. Similarly, the case $i=3$, for which the smallest stable island is a tetramer, was studied on a two-dimensional square substrate by using the assumption that atoms with two or more nearest-neighbor bonds were immobile while atoms with fewer bonds were assumed to diffuse at the same rate.

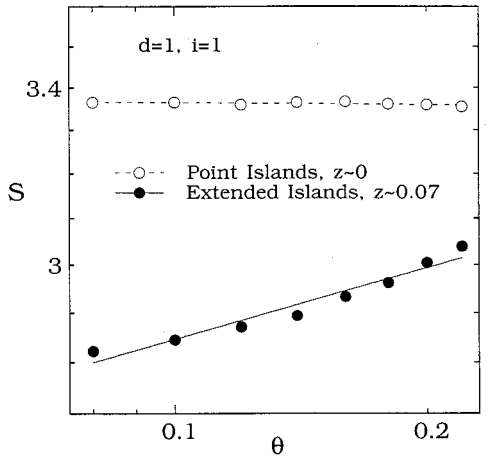

FIG. 1. The variation of the average island size with coverage in the saturated lattice for both extended-island and point-island models in one dimension and with $i=1$.

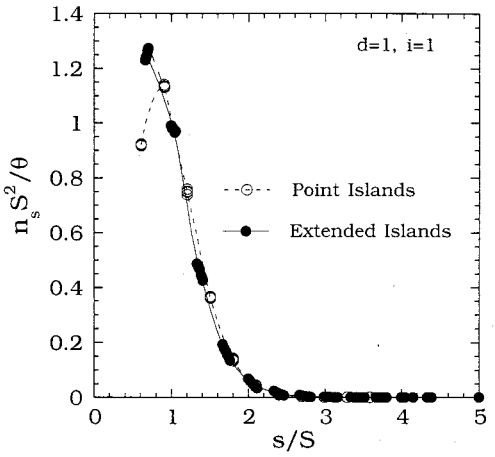

FIG. 2. Scaled island size distributions for a coverage range of $0.1 \leqslant \theta \leqslant 0.2$ for the extended-island and point-island models in one dimension, for $i=1$.

We note that this definition of critical island size is more physical than that used in the point-island model (for which any site containing $i+1$ or more particles corresponds to a stable island), since it takes the bonding geometry into account.

In order to determine the scaling behavior at saturation, the island density n, average island size $S=\theta/n$, and island-size distribution $n_s(\theta)$ [where $n_s(\theta)$ is the density of islands of size s at coverage θ] were measured as functions of coverage at the end of the nucleation process when only stable clusters remain. In our analysis of the island-size distribution $n_s(\theta)$ we assumed the dynamic scaling form[17,22]

$$n_s(\theta)=\theta S^{-2} f\left(\frac{s}{S}\right), \quad s \geqslant 2, \tag{1}$$

where the scaling function $f(u)$ is assumed to be independent of coverage. The use of this scaling form is based on the assumption that there is only one relevant length scale or size corresponding to the average island size. For deposition on a one-dimensional substrate lattices of size $L=10^4$ were used while in two dimensions we used lattices of lateral size $L=128$ and 256. Periodic boundary conditions were used and the results were averaged over at least 500 runs.

III. RESULTS

Figure 1 shows our results for the average island size S as a function of coverage for the case $i=1$ on a one-dimensional substrate, along with the corresponding point-island results. As expected, for the point-island model, the average island size S is independent of coverage i.e., $S \sim \theta^z$ with $z=0$.[26] However, for the more realistic extended-island model the average island size increases with increasing coverage, leading to a nonzero effective value of z ($z_{\text{eff}} \simeq 0.07$ for $0.1<\theta<0.2$) while the effective exponent actually increases with coverage. The increase in z with coverage is due to the increased probability of coalescence with increasing coverage for extended islands.

Figure 2 shows the corresponding scaled island-size distributions over the same range of coverage. As can be seen, although there is a significant difference in the scaling behavior of the average island size between the point-island and extended-island models, the scaled island-size distributions are very similar.[27] In particular, both island-size distributions decrease monotonically and are almost identical for $s/S>1$, which corresponds to $s \geqslant 3$. We note that our use of the scaling form (1) is more appropriate than the form $n_s(\theta)=\theta^{1-2z} g(s/\theta^z)$ used in Ref. 26 because it does not require the assumption of a constant value of the exponent z.

We now consider the scaling of the island density and size distribution for the case of deposition on a two-dimensional substrate with $i=1$. Figure 3 shows a log-log plot of the average island size as a function of coverage for this case for both point and extended islands. For the point-island case the rates of nucleation and aggregation are essentially the same at all coverages. This leads to an average island size S that is independent of coverage and to an exponent $z \simeq 0$. In contrast, for the extended-island model the average island size

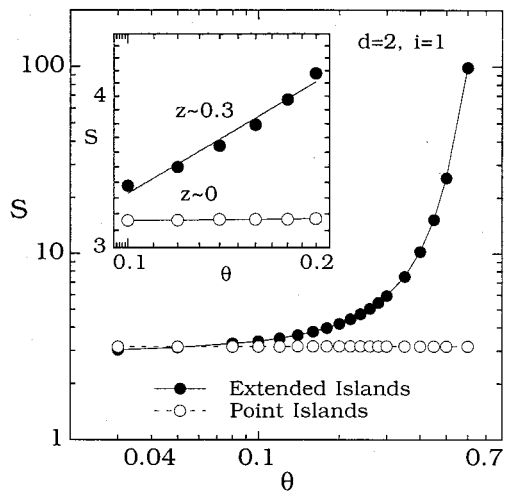

FIG. 3. Average island size S in the saturated lattice as a function of coverage for the extended-island and point-island models in two dimensions and with $i=1$. The inset shows an approximate scaling behavior for $\theta \leqslant 0.2$.

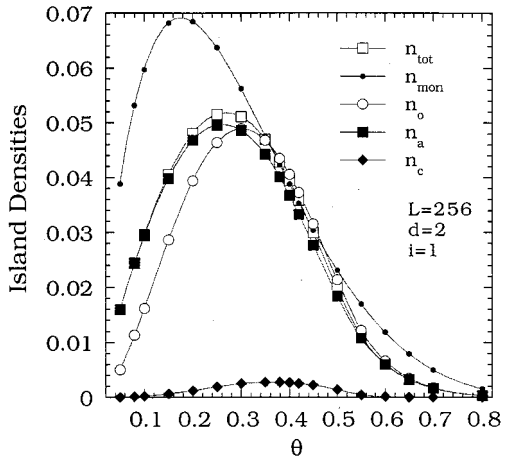

FIG. 4. The dependence of various island densities on coverage: the total island density in the saturated lattice n_{tot}, the initial nuclei density n_0, the density of islands in the saturated lattice grown only by nucleation and aggregation n_a, the density of islands in the saturated lattice that underwent diffusion coalescence n_c, and the density of monomers n_{mon} immediately after deposition.

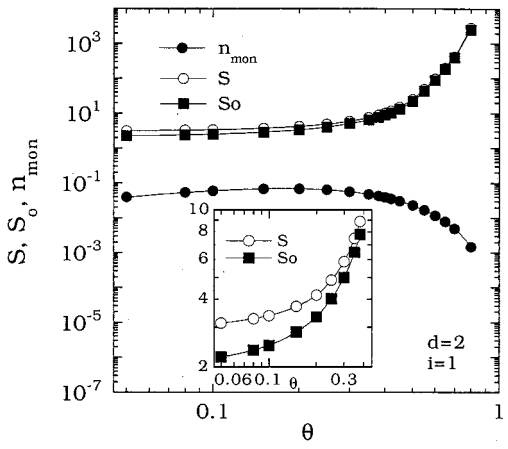

FIG. 5. Average island size S_0 and monomer density n_{mon} immediately after deposition and the average island size in the saturated lattice S as a function of coverage. The inset shows a detail of the S,S_0 plot at low coverages.

increases rapidly with increasing coverage. The increase in average island size with increasing coverage occurs due to coalescence just as in one dimension. We note that this increase begins well before the percolation threshold, which we measure to be $\theta_p \simeq 0.53$, slightly lower than the random-site percolation threshold $p_c = 0.59$. The inset indicates that for $0.1 < \theta < 0.2$ the increase of the island size with coverage may be described by an effective exponent $z_{\mathrm{eff}} \simeq 0.3$.

As for the case of deposition on a one-dimensional substrate, the increase in z with coverage for extended islands is due mainly to the increased rate of coalescence with increasing coverage. This effect is more pronounced than in one dimension, since as the surface covered by an island increases the probability of coalescence events increases more rapidly. In two dimensions the increase in the island capture number with island size also plays a role at low and intermediate coverage since it tends to emphasize aggregation or growth of existing islands over nucleation. Since these effects become stronger with increasing coverage they also contribute to an effective value of z that increases with coverage as shown in Fig. 3.

To quantify the effects of coalescence on island density, in Fig. 4 we show how the various island densities change with coverage, in the saturated lattice. For $\theta < 0.28$ the total island density n_{tot} increases with increasing coverage, due to enhanced nucleation. However, at higher coverages island coalescence leads to a steady decrease in the island density. The coalescence of islands occurs in two steps: during deposition and after deposition. The first step determines the initial postdeposition island density and size distribution, before the onset of particle diffusion. As particles are being deposited, they nucleate new islands, aggregate to existing ones, or bridge two or more islands. After deposition, hopping adatoms will lead to the same three processes of nucleation, aggregation, and coalescence.

The total island density n_{tot} in the saturated lattice is the sum of n_a (the density of islands that after deposition grew only by nucleation and aggregation) and n_c (the density of islands that underwent coalescence as a result of particle diffusion). The density n_c of islands that coalesced by diffusion peaks at a coverage $\theta \simeq 0.38$, while the density n_a of islands that never coalesced after deposition follows closely the behavior of the total island density, differing only within the coverage range for which the increase in diffusion coalescence is more significant, $\theta = 0.2 - 0.5$. Also shown in Fig. 4 are the density n_0 of nuclei formed immediately after deposition and the initial density of monomers n_{mon}, as a function of coverage. As can be seen, n_0 is close to n_{tot} for all coverage values. This indicates that the main effects of coalescence occur during deposition rather than during diffusion.

To illustrate this more clearly, we show in Fig. 5 a comparative plot of the average island size S_0 immediately after deposition, as well as the average island size S in the saturated lattice. The density of monomers immediately after deposition is also shown. As can be seen, the final average island size is close to the initial average island size for most coverages and they almost coincide for high coverages. The main differences between them occur mostly for coverages below 0.38, where the density of monomers after deposition is fairly large and they can contribute to a change in S mainly by aggregating to the existing islands. Since for larger coverages the average island size in the saturated lattice is very close to the average island size immediately following deposition, most of the coalescence occurs while particles are being deposited, rather than later, by diffusion.

In Fig. 6 we show the fractions of the total number of islands that did or did not coalesce by diffusion, and how these fractions change with coverage. The results show that after deposition most islands have never coalesced. However, the fraction n_a/n_{tot} of islands that have not coalesced through diffusion decreases slightly with increasing coverage—and, accordingly, the fraction n_c/n_{tot} of islands that coalesced during diffusion increases slightly with increasing coverage—until the coverage reaches the percolation threshold $\theta \simeq 0.53$. Once percolation occurs, the fraction of islands that never underwent postdeposition coalescence goes up again, to form almost all of the islands.

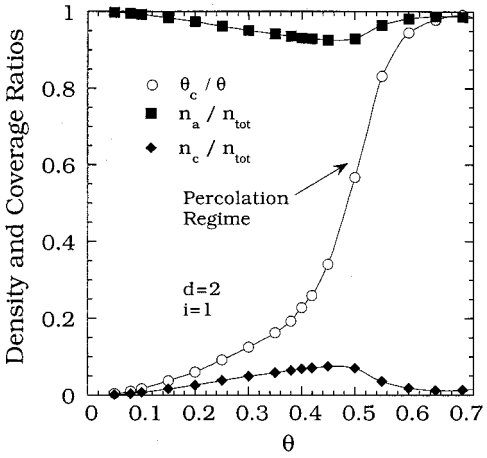

FIG. 6. The variation with coverage of the fraction of the total island density n_a/n_{tot} that grew through nucleation and aggregation only, compared to the fraction of islands n_c/n_{tot} that coalesced after deposition. Also shown is the variation with coverage of the fraction of the total coverage contained in islands that underwent diffusion coalescence.

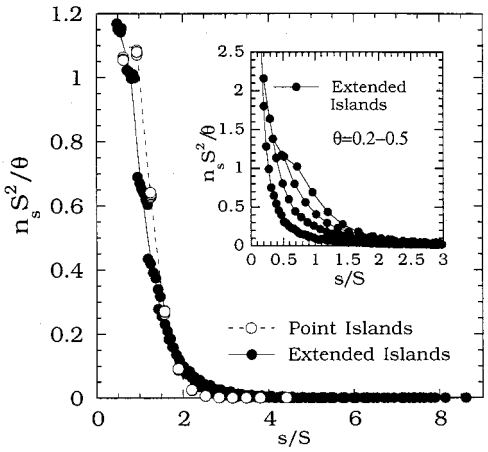

FIG. 7. Scaled size distributions for $\theta \leqslant 0.2$ for the extended-island and point-island models in two dimensions, for $i=1$. The inset shows the breakdown in scaling for extended islands, at coverages above 0.2.

This behavior is explained in the same figure by plotting the fraction of the total coverage contained in islands that underwent diffusion coalescence as a function of coverage. We see that the number of particles belonging to postdeposition-coalesced islands keeps increasing slowly with coverage until the percolation threshold is reached. At this point this number increases dramatically as the percolating cluster, grown by coalescence, contains a significant amount of particles. Above this coverage, more and more particles become part of this surface-spanning cluster, until all islands have merged into one large island.

Thus, Fig. 6 shows that most of the deposited particles are accumulated in only a few large islands that have grown by coalescence. Therefore, at low coverage the differences between the point-island and extended-island models are caused by the initial distribution as well as by the diffusion process. However, at higher coverage ($\theta > 0.4$) most differences originate in the lattice configuration immediately following deposition.

We now consider the scaled island-size distribution for both point and extended islands, as shown in Fig. 7. As can be seen, for $\theta < 0.2$ the scaled point- and extended-island-size distributions are similar and closely resemble those obtained in one dimension. However, as the inset shows, for $\theta > 0.2$ scaling breaks down for the extended-island model due to coalescence. Thus, the use of a realistic extended-island model strongly affects both the scaling behavior of the average island size and the island-size distribution for intermediate and large coverages.

Figure 8 reemphasizes the dependence of the initial island-size distribution on the island geometry. As can be seen, the way in which the two models interpret the initial particle distribution on the lattice becomes of crucial importance for the subsequent island growth. Since nearest neighbors are treated as part of the same island in the extended-island model, but belong to different islands in the point-island model, the initial lattice is viewed very differently in the two models. Also, as shown, whether or not particles are allowed to land on top of each other leads to further differences in the initial lattice configuration.

In Fig. 9 we compare the kinetic Monte Carlo results for point and extended islands to the island distributions obtained through mean-field calculations, by solving the rate equations[28]

$$\frac{dn_1}{dt} = -2\sigma n_1^2 - \sigma n_1 n, \tag{2}$$

$$\frac{dn_s}{dt} = \sigma n_1 (n_{s-1} - n_s). \tag{3}$$

In these equations, n_s is the density of islands of size s ($s \geqslant 2$), n_1 is the monomer density, n is the total island density, and σ is the capture number (or reaction rate). A constant capture number was used for the point-island case, while for the extended-island case we used a size-dependent capture

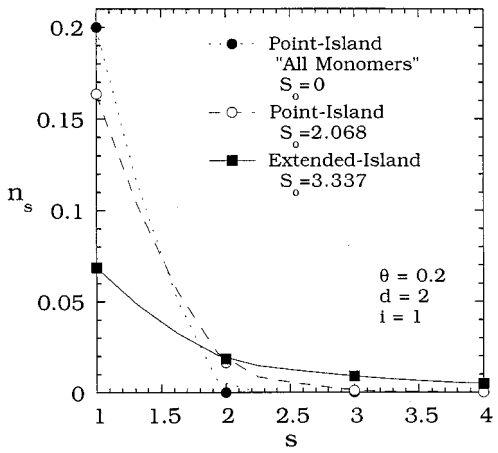

FIG. 8. Island-size distributions calculated for the extended-island model and the point-island model immediately after deposition. Also shown (filled circles) are results for a modified point-island model that does not allow particles to land on top of other particles.

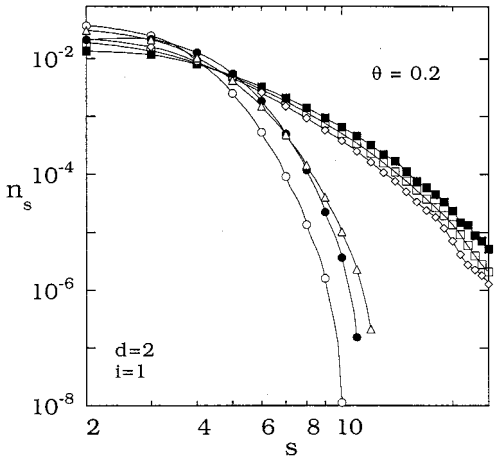

FIG. 9. Island-size distributions obtained from mean-field calculations (open symbols) along with the corresponding kinetic Monte Carlo results (filled symbols), for the point- and extended-island models, for $d=2$ and $i=1$, at $\theta=0.2$. Squares correspond to extended islands, circles correspond to point islands, triangles correspond to extended islands with an all-monomer initial distribution, and diamonds correspond to point islands with extended-island initial distribution.

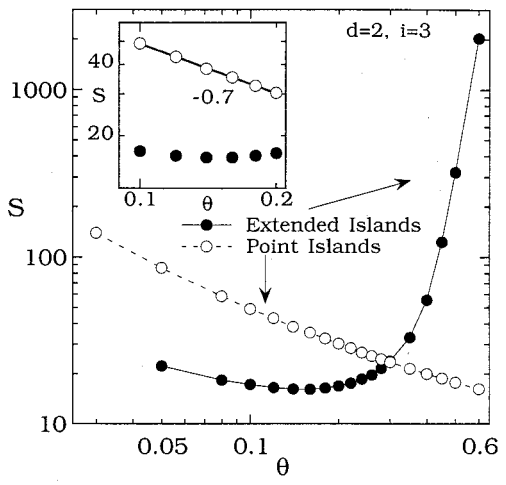

FIG. 10. Average island size S in the saturated lattice as a function of coverage for the extended-island and point-island models in two dimensions, for $i=3$.

number $\sigma=\sqrt{s}$. Also, to evaluate the importance of the lattice configuration immediately after deposition, we used various initial conditions for both point- and extended-island models, at a coverage of $\theta=0.2$. We see that there are two clearly separated groups of results: the Monte Carlo island distribution for the point-island case is close to the results obtained by using a point-island initial distribution (we used both an all-monomer initial distribution and a distribution that considers some initial islands larger than $s=1$, due to deposition on top of other particles), regardless of the capture number used. Similarly, for the extended-island case, the Monte Carlo results compare best to the mean-field results obtained starting with the extended-island initial distribution, depending only weakly on the type of capture number used, as the inset shows.

These results reinforce the earlier findings that the main reason for the difference between the point- and extended-island results in $d=2$ with $i=1$ is the initial, postdeposition island distribution. This suggests an intermediate solution in simulating island growth in this case, consisting of a correctly read initial lattice configuration, further allowed to evolve using the point-island approximation. This approach will provide a realistic final lattice, both by Monte Carlo simulations and by mean-field calculations, while the degree of difficulty of the computations involved is much less than in a fully extended-island approach.

We now consider the dependence of the average island size on deposition coverage for the case $i=3$ in $d=2$ as shown in Fig. 10. For point islands the average island size decreases with increasing coverage ($z\simeq-0.7$).[26] However, for the more realistic extended-island model the island size decreases much more weakly at low coverage and then increases for $\theta>0.15$. For both models the decrease in island size at low coverage is due to the rapid increase in nucleation with increasing coverage for $i=3$. However, for the extended-island model the average island size increases with coverage for $\theta>0.15$ due to enhancement of coalescence and, to a lesser extent, to the increase in the capture number with increasing island size.

Figure 11 shows the corresponding results for the island-size distribution at $\theta=0.2$ for the case $i=3$ in $d=2$. For the point-island model the distribution is smooth and has a clear peak. However, for the extended-island model an island is not completely immobile until its constituent particles each have two or more nearest neighbors. As a result some ''magic'' island sizes are preferred over others, leading to oscillations in the island-size distribution, superimposed over a generally decreasing trend.

The occurrence of the ''magic'' sizes can be understood in terms of the probabilities that a given island size is stable. The larger the number of possible configurations that allow all constituent particles to have two or more nearest neighbors for a given island size, the higher is the frequency of occurrence of islands of that size in the final lattice. Also, the larger the minimum number of particles needed to be added

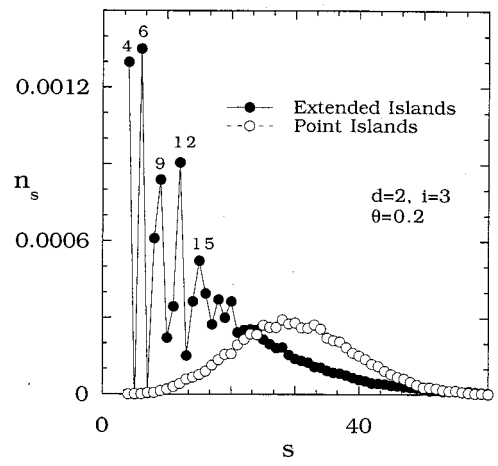

FIG. 11. A comparison between the island size distribution for the extended-island and point-island models, at a coverage of 0.2, in two dimensions and for $i=3$.

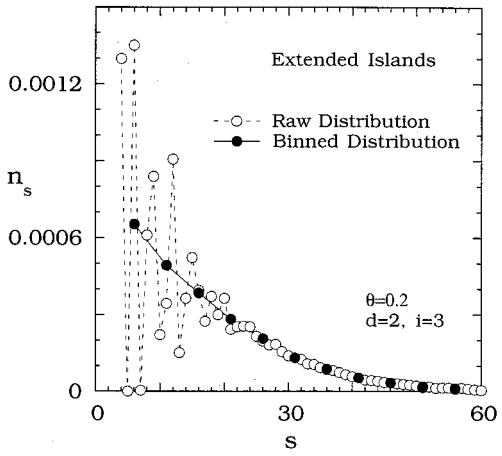

FIG. 12. Binned size distribution for the extended-island model in two dimensions and for $i=3$ at a coverage of 0.2.

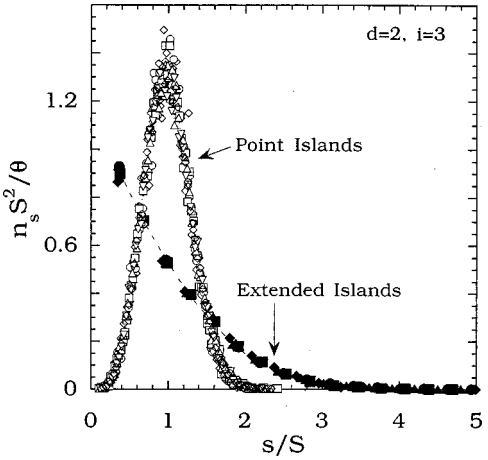

FIG. 13. Scaled size distributions for a coverage range of $0.1 \leqslant \theta \leqslant 0.2$, for both the extended-island and point-island models in two dimensions, for $i=3$.

to a stable island of a given size to form a larger stable island, the higher the chances for islands of that size to occur in the final lattice. In contrast, islands that have a large number of unoccupied ''edge'' sites with two nearest neighbors (i.e., kink sites) will occur with a lower probability. Finally, islands of sizes that are multiples of $i+1=4$ are more probable since they can be formed by coalescence of nucleus islands of size $i+1=4$. The final size distribution is the result of the combined action of all these factors. We note that a correct rate-equation description of this behavior would thus have to assign proper capture numbers to each island according to its so called perimeter polynomials,[29] which depend on both the island size and perimeter, and for which there is no exact solution.

In order to scale the island-size distribution for the extended-island model with $i=3$ in $d=2$ the raw size distributions were first binned, using a bin size of 5, as shown in Fig. 12 in order to remove the oscillations. The resulting smoothed distributions were then scaled using Eq. (1) for different coverages as shown in Fig. 13. Also shown are the corresponding scaled distributions for point islands. As can be seen both distributions exhibit excellent scaling. However, as already noted, while the point-island size distribution is sharply peaked,[26] for extended islands the smoothed island-size distribution decreases monotonically. Thus, for the case $i=3$ in $d=2$ the island geometry leads to a strong difference in the two distributions.

IV. DISCUSSION

In this paper we investigated the scaling of the submonolayer island density and island-size distribution for the case of postdeposition nucleation using an extended-island model with realistic geometry. Our results show that except at extremely low coverages the use of a realistic island geometry leads to significant differences in the coverage dependence of the average island size as well as in the corresponding exponent z in comparison to the point-island model. In particular, for the case $i=1$ we find that the average island size increases rapidly with coverage in both one and two dimensions, leading to a nonzero effective value of z, which increases with increasing coverage. The increased value of z for extended islands is due mainly to the enhancement of coalescence due to island geometry that occurs primarily during the deposition process, rather than to the increase in the capture number with the island size. In contrast, the effects of island geometry lead to only a small change in the scaled island-size distribution, at least at low and intermediate coverages. However, at higher coverages coalescence also leads to a modified size distribution and a breakdown in scaling.

We have also presented results for postdeposition nucleation in two dimensions for $i=3$. In this case, not only did the effects of island geometry lead to significant differences in the scaling of the average island size but there were also significant differences in the island-size distribution even at low coverages. In particular, for the point-island case, the island-size distribution is peaked as in ordinary deposition.[15] In contrast in the case of extended islands there is no clear peak although oscillations were observed. As already noted, these oscillations in the size distribution are due to the existence of magic island sizes which occur as a result of the realistic island geometry.

In conclusion, we have shown that island geometry plays an important role in postdeposition nucleation and growth. In particular, the use of a model with realistic island geometry leads to a significant enhancement in the average island size as well as changes in the scaled island-size distribution for sufficiently large coverage. In addition, for $i=3$, the inclusion of the correct bonding geometry leads to significant changes in the scaled island distribution. We expect that these results will be useful in the interpretation of experiments on postdeposition island growth.

ACKNOWLEDGMENTS

This work was supported by grants from the National Science Foundation and the Office of Naval Research.

[1] R. Q. Hwang, J. Schroder, C. Gunther, and R. J. Behm, Phys. Rev. Lett. **67**, 3279 (1991).
[2] J. A. Stroscio and D. T. Pierce, Phys. Rev. B **49**, 8522 (1994).
[3] J. A. Stroscio, D. T. Pierce, and R. A. Dragoset, Phys. Rev. Lett. **70**, 3615 (1993).
[4] D. D. Chambliss and K. E. Johnson, Phys. Rev. B **50**, 5012 (1994).
[5] H. J. Ernst, F. Fabre, and J. Lapujoulade, Phys. Rev. B **46**, 1929 (1992).
[6] H.-N. Yang, G.-C. Wang, and T.-M. Lu, Phys. Rev. Lett. **73**, 2348 (1994).
[7] J.-K. Zuo and J. F. Wendelken, Phys. Rev. Lett. **66**, 2227 (1991).
[8] J.-K. Zuo, J. F. Wendelken, H. Durr, and C.-L. Liu, Phys. Rev. Lett. **72**, 3064 (1994).
[9] Y. W. Mo, J. Kleiner, M. B. Webb, and M. G. Lagally, Phys. Rev. Lett. **66**, 1998 (1991).
[10] W. Li, G. Vidali, and O. Biham, Phys. Rev. B **48**, 8336 (1993).
[11] M. Zinke-Allmang, S. C. Puddephatt, and T. D. Lowes, Proc. SPIE **2140**, 36 (1994).
[12] P. Smilauer, M. R. Wilby, and D. D. Vvedensky, Phys. Rev. B **47**, 4119 (1993).
[13] G. S. Bales and D. C. Chrzan, Phys. Rev. B **50**, 6057 (1994).
[14] J. G. Amar, F. Family, and P. M. Lam, Phys. Rev. B **50**, 8781 (1994).
[15] J. G. Amar and F. Family, Phys. Rev. Lett. **74**, 2066 (1995).
[16] A. F. Voter, Phys. Rev. B **34**, 6819 (1986).
[17] T. Vicsek and F. Family, Phys. Rev. Lett. **52**, 1669 (1984).
[18] J. A. Blackman and P. Mulheran, Phys. Rev. B **54**, 11 681 (1996).
[19] L.-H. Tang, J. Phys. I **3**, 935 (1993).
[20] F. Family and P. Meakin, Phys. Rev. A **40**, 3836 (1989).
[21] F. Family and P. Meakin, Phys. Rev. Lett. **61**, 428 (1988).
[22] M. C. Bartelt and J. W. Evans, Phys. Rev. B **46**, 12 675 (1992).
[23] Y. Okada, J. S. Harris, Jr., A. Sutoh, and M. Kawabe, in *Evolution of Epitaxial Structure and Morphology*, edited by A. Zangwill, D. Jesson, D. Chambliss, and R. Clarke, Mater. Res. Soc. Symp. Proc. No. 399 (Materials Research Society, Pittsburgh, 1996), p. 203.
[24] B. Muller, L. Nedelmann, B. Fischer, H. Brune, and K. Kern, Phys. Rev. B **54**, 17 858 (1996).
[25] G. Rosenfeld, R. Servaty, C. Teichert, B. Poelsema, and G. Comsa, Phys. Rev. Lett. **71**, 895 (1993).
[26] J. Li, A. G. Rojo, and L. M. Sander, Phys. Rev. Lett. **78**, 1747 (1997).
[27] The slightly different behavior for small island size is most likely due to minor differences between our point-island model and the one used in Ref. 26.
[28] We thank M. N. Popescu for the help with the numerical integration of these equations.
[29] D. Stauffer, *Introduction to Percolation Theory* (Taylor and Francis, London, 1985), pp. 25–26.